frontiers in Physics

ORIGINAL RESEARCH
published: 14 January 2021
doi: 10.3389/fphy.2020.614684

Physicochemical Properties of Pure Water Treated by Pure Argon Plasma Jet Generated by Microwave Discharge in Opened Atmosphere

*Konstantin F. Sergeichev[1], Natalya A. Lukina[1], Ruslan M. Sarimov[1], Igor G. Smirnov[2], Alexander V. Simakin[1], Aleksey S. Dorokhov[2] and Sergey V. Gudkov[1]**

[1]*Prokhorov General Physics Institute of the Russian Academy of Sciences, Moscow, Russia,* [2]*Federal State Budgetary Scientific Institution "Federal Scientific Agroengineering Center VIM" (FSAC VIM), Moscow, Russia*

The physicochemical properties of water activated by high-purity low-temperature argon plasma of electrodeless microwave discharge at atmospheric pressure are investigated. Such parameters of activated water as electrical conductivity, redox potential, hydrogen index (pH), the concentrations of dissolved molecular oxygen, hydrogen peroxide, OH-radicals, nitrate and nitrite anions depending on the plasma jet distance above the water surface and duration of activation were studied. Under irradiation conditions close to optimum, it was shown that the generation rate in the absence of impurities are 200 μM/min for H_2O_2; 800 μM/min for $^{\bullet}OH$ and 2 mM/min for NO_x^-. The use of plasma activated water (PAW) in agriculture has been tested. It was shown that strawberry seeds treated with a surfactant solution grow much faster than control seeds. The mechanisms of the chemical composition formation of activated water and its biological properties are discussed.

Keywords: low-temperature argon plasma, plasma activated water, PAW, reactive oxygen species, ROS, agriculture, growth and development of plants

OPEN ACCESS

Edited by:
Francesco Caravelli, Los Alamos National Laboratory (DOE), United States

Reviewed by:
Denis Yanykin, Institute of Basic Biological Problems (RAS), Russia
Alex Sergeevich Chernov, Institute of Bioorganic Chemistry (PAS), Poland

****Correspondence:***
Sergey V. Gudkov
s_makariy@rambler.ru

Specialty section:
This article was submitted to Interdisciplinary Physics, a section of the journal Frontiers in Physics

Received: *06 October 2020*
Accepted: *18 November 2020*
Published: *14 January 2021*

Citation:
Sergeichev KF, Lukina NA, Sarimov RM, Smirnov IG, Simakin AV, Dorokhov AS and Gudkov SV (2021) Physicochemical Properties of Pure Water Treated by Pure Argon Plasma Jet Generated by Microwave Discharge in Opened Atmosphere. Front. Phys. 8:614684. doi: 10.3389/fphy.2020.614684

INTRODUCTION

Water treated with Low-Temperature (LT) plasma in an open atmosphere acquires specific properties due to the formation of short- and long-lived chemically reactive species of oxygen and nitrogen (RONS) [1]. Reactive oxygen species (ROS) are formed as a result of oxygen electron transfer reactions and become the main molecular participants in redox reactions. Among them there are superoxide anion radical ($O_2^{\bullet-}$), hydrogen peroxide (H_2O_2), singlet oxygen ($^1O_2$), ozone (O_3), hydroxyl radical ($OH^{\bullet}$), hydroperoxide radical ($HO_2^{\bullet}$), and also the reactive nitrogen species (RNS), i.e., nitric oxide ($NO^{\bullet}$), which in water solutions forms nitrous acid (HNO_2) and nitric acid (HNO_3) at in reactions with ROS forms an effective oxidizing agent, peroxynitrite $ONOO^-$ [2]. Due to its powerful bactericidal properties, plasma activated water (PAW) is used in many areas of life: in agriculture, ecology, food production and biomedicine. In "plasma medicine," the culture medium (plasma activated media [PAM]) obtained by the PAW treatment methods showed a strong antitumor effect on various types of cells [3], such as lung cancer, adenocarcinoma and human breast cancer cells [4]. In plant biology, PAW has been found to be very effective as a stimulator of seed germination, an environmentally friendly bactericidal and fungicidal antiseptic [5]. It is known that, thanks to enzymes (NADH-oxidases), hydrogen peroxide H_2O_2 is generated in the plants themselves to fight diseases and phytopathogens. If hydrogen peroxide comes from outside, it causes

an alarm and mobilizes the plant's immunity to counter stress and besides kills microorganisms with atomic oxygen after decomposition. At a concentration of 0.001–0.1% at room temperature, H_2O_2 inhibits the growth of microorganisms, and at a concentration of 0.1% or higher it acts as a bactericide or fungicide [6]. Seeds treated with H_2O_2 solution before sowing are characterized by increased germination, and the plants become resistant to adverse weather conditions (drought, soil salinization, etc. [7, 8]) and less susceptible to fungal diseases [9].

Sources of LT plasma for use in biology and medicine should preferably work *in vivo*, i.e., at atmospheric pressure. Such sources have been intensity developed in the last 3 decades. Hundreds of works and a number of reviews are presented on this subject [10–17]. LT plasma is now widely used in almost all areas of the natural sciences: physics and chemistry [18, 19], biology and medicine [1, 16], technology [20], in foods production and agriculture [21–23].

The methods for producing LT plasma in atmosphere (*in vivo*) for biomedical applications are very diverse [24, 25]. A discharge in an electric field in an open atmosphere is not used, since it requires a high field strength: more than 30 kV/cm. A significant number of methods for producing LT plasma are based on self-sustaining direct current arc discharge (DCAD) [26]. This discharge has a low cathode potential drop of ~10 V and does not require high-voltage power supplies. At the same time, the discharge has a high current density, a high plasma density $\sim 10^{17}\,cm^{-3}$ and an ultrahigh temperature of ~10,000 K. Arc plasma is used in the technique of welding, metal cutting and solid waste processing. That plasma temperature is unacceptable for medical use, however, this obstacle is overcome with the help of the so-called atmospheric pressure plasma jets that work on some medical devices. We give examples of the arc jets. In a dense arc discharge plasma, many different active particles is generated, which can be used to activate biological media and water by passing an air stream through an interelectrode space with the plasma [27]. The discharge is carried out in a small volume insulated by a dielectric sleeve between two flat electrodes with a narrow gap of 0.5 mm and orifices of 0.2 mm through which air is blown. An air jet cools the plasma and removes charged particles and radicals from the plasma that can activate water and biological media. Another example of using AD is implemented in [28], where direct synthesis of H_2O_2 in water is carried out under the influence of argon plasma on it. Argon is blown down through a tubular electrode onto the surface of the water, and water moves up toward the argon flow coaxially through another tubular electrode. In a gap of 3 mm wide between the electrodes, an atmospheric pressure arc discharge is ignited from a 500 V direct current source. Water must be an electrolyte (for instance, saline) so that a continuous current can flow through the water boundary. The synthesis of hydrogen peroxide H_2O_2 in this device is a consequence of the transfer of plasma charges to water. At the same time, sputtering, emission of hydrated ions and evaporation caused by electric discharge occur on the water surface. In the following example, the formation of PAW or PAM were investigated under the influence of a direct current plasma jet of mixture of He-O_2 gases, which incident on deionized water or biological media in the open atmosphere or in a closed chamber, and the ability of such plasma jet to inactivate bacteria were studied [29]. The gas mixture is passed down through a quartz tube with an inner diameter of 4 mm, on the axis of which there is an electrode in the form of a stainless steel needle with a diameter of 1 mm, to which a high voltage is applied. The tip of the needle of the high voltage electrode is 10 mm above the end of the quartz tube, and a grounded ring electrode 10 mm high is put on the tube opposite the end of the needle. A plasma jet, propagating from the needle electrode, touches the surface of the fluid being treated.

A common drawback of numerous DCAD inkjet sources is the direct contact of the plasma with metallic electrodes that break down and pollute water or media with metal oxides, which become catalysts for the decomposition of H_2O_2 and pollute the media or water by reactive metall particles generated by electrode micromelting [30]. The consequence of the small size of the discharge systems is their low productivity and operational unreliability. Systems designed for plasma treatment of aqueous electrolytes have a limited scope of their medical application.

Barrier discharges (DBDs) [31] and corona discharges [32] are also common methods for producing "cold" plasma. DBD operate in the mode of self-breakdown in high voltage alternating fields. The typical electron temperature DBD is several eV, while the gas temperature is close to room temperature. The peak electron concentration is of order $10^{11}\,cm^{-3}$. The disadvantage of the DBD method is that plasma generation occurs near the dielectric surface, which undergoes erosion under the influence of plasma particles. Corona discharges are powered by high voltage at extremely low current densities of ≤200 μA. A needle in a corona discharge also undergoes plasma erosion, which does not allow us to consider these methods as pure enough for medical use. Installations of an electrodeless discharge excitation by radio-frequency, microwave, and laser sources of electromagnetic radiation are an exception to most installations of plasma activation. However, electrodeless radio-frequency sources of inductively coupled plasma, which are widely apply in optical emission spectroscopy to analyze the gas (vapor) composition [33], use quartz or ceramic tubes, through which plasma is blown out by stream of ionized gas, what can also pollute the plasma with the products of the tube material atomization.

The problem of purity PAW and PAM concerns, of course, not only the plasma, but also the water being activated. For plasma treatment, water of various degrees of purification is used: industrial water, drinking water, distillate, double distillate, deionized water and physiological saline. The purpose of this work is to show the possibility of nonequilibrium atmospheric pressure argon plasma (N-APPJs), generated by a microwave jet source for producing pure PAW for biomedical applications. The purity of PAW should be determined by the purity of water and the purity of the plasma obtained by the electrodeless transfer of microwave energy into the plasma.

EXPERIMENTAL SECTION

Microwave Device for Plasma Activation of Liquids

A sketch of a device, elaborated on the basis of a microwave plasmatron operating in the atmosphere is shown in **Figure 1**. A

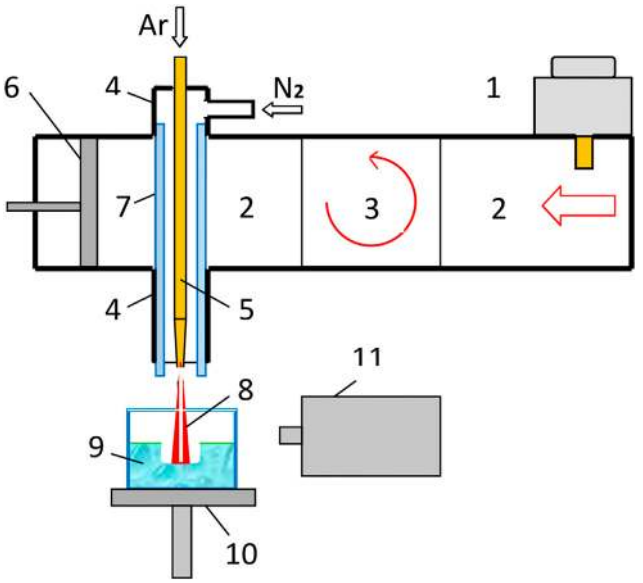

FIGURE 1 | Schematic diagram of the microwave device for plasma activation of liquids: 1–magnetron Samsung OM75P (31), 2–rectangular waveguide of a cross-section (45 × 90 mm^2), 3–ferrite isolator, 4–coaxial waveguide, 5–central conductor of the coaxial line with a nozzle at its end, 6–tuning piston, 7–quartz pipe, 8–plasma jet, 9–water target in a quartz cell, 10–cell holder, 11–spectrometer AvaSpec-3648-USB2.

continuous generation mode magnetron of 0.9 kW power and oscillation frequency of 2.45 GHz is used as microwave source [34]. The microwaves propagate from the magnetron (1) through a rectangular waveguide (2) of the cross section 45 × 90 mm^2, then go through a ferrite isolator (3) to a waveguide-coaxial transforner, where the TM_{10}-mode of a rectangular waveguide is converted into the TEM-mode of the coaxial waveguide (4, 5). The isolator is a magnetron protection against reflected microwave power before ignition of a discharge. Microwave power transmission from the magnetron to gas discharge, as a load, is matched by a tuning piston (6). A copper pipe of 6 mm diameter is a central conductor (5) of the coaxial waveguide with a pointed tip-nozzle with bore of 1.5 mm diameter. Argon is supplied through the pipe and flows out the nozzle as a directed jet, while slightly expanding. The coaxial screen of the waveguide (4) between the walls inside the rectangular waveguide (2) is removed for coupling between the waveguides via the conductor (5). The working space of the coaxial waveguide is separated from the rest waveguide space by a radio-transparent quartz tube (7). Buffer gas (nitrogen) is blown through the tube around the argon jet (7) for stabilization of discharge burning and for to prevent a transverse breakdown between the nozzle and the coaxial screen edge (4). The argon jet (8) in a result of ionization under the influence of a microwave field, becomes the plasma jet, which flows down vertically from the nozzle, that us allows to use in experiments a liquid targets in an open vessel (9).

The argon jet flows out the nozzle at a high directional speed of ~30–50 m/s (gas flow rates 3–5 L/min) at the pressure slightly more than 1 atm. The plasma jet is detached off the nozzle by an neutral argon stream due to the gas jet speed is more than the speed of ionization front propagation along the gas jet toward the nozzle. Therefore, a gap of neutral argon between the plasma jet and the nozzle is formed. Since the nozzle (7) does not have direct contact with the plasma jet, it is not heated and not vaporized by the plasma, what allows us to consider the discharge as electrodeless. Microwave power is transmitted through the coaxial waveguide to the plasma jet owing to capacitive coupling between the nozzle and plasma. The diameter of most brightly glowing "rod" of the plasma jet is no more than 0.2–0.3 cm, The rod length does not exceed a quarter of the wavelength of microwave radiation, $\lambda/4 \approx 3$ cm, what is determined by laws of electrodynamics. The electron temperature is ~1,5 eV, the gas temperature is ~4000 K. A brightly glowing rod (**Figure 2**) carries ions and excited argon atoms onto the water surface with a high directed velocity. The water is treated in an quartz cell with volume of 0,1 L (9), which is placing on the elevator (10), see **Figure 1**, which allows varying the distance from the water surface to the nozzle. The gas-dynamics pressure of argon stream creates a pit on the water surface of dimensions a 1.5 cm diameter to a depth of 1.5 cm (**Figure 2**). Ultraviolet radiation of the plasma jet is second factor acting on water, which creates a halo of excitation and photoionization of ambient gases around the plasma rod, including nitrogen and water vapor (**Figure 2**).

Deionized water is an object of the plasma activation. The luminous end of the plasma jet might be in contact with the water surface and also might be immersed into it. Chemical reactions occur inside a pit due to interaction of water and the jet of nonequilibrium plasma. Optical emission spectra of the plasma jet were studied with a spectrometer AvaSpec-3648-USB2, calibrated by a manufacturer in the wavelength range 360–940 nm, with resolution of 0.3 nm.

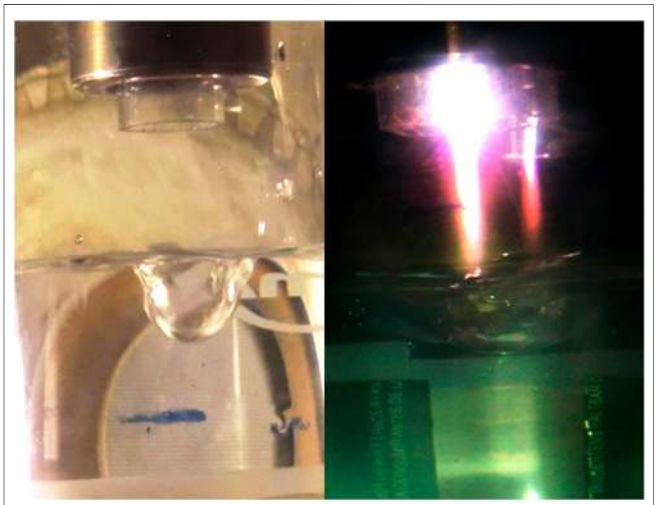

FIGURE 2 | View of a pit on the water surface formed with the gas dynamic pressure, before microwave power switch on (picture on left). View of a microwave plasma jet after plasma ignition (on right). A brightly glowing torch rod is surrounded by a less bright halo of photoionization of nitrogen, steam and air. Behind, it is seen the torch reflection in the wall of the cell.

Physicochemical Methods of Investigation

The physical and chemical characteristics of the solutions were determined no later than 1 h after treatment. Detection of hydrogen peroxide production. A highly sensitive enhanced chemiluminescent technique based on luminol-*p*-iodophenol-horse radish peroxidase was used for detection and quantification of hydrogen peroxide in aqueous solutions. The luminescence was detected with Biotoks-7AM chemiluminometer (Econ, Russia). The concentration of the produced hydrogen peroxide was calculated from the calibration curves plotted by the measured values of chemiluminescence intensity of the templates containing the added hydrogen peroxide in a particular concentration [35]. The initial concentration of H_2O_2 used for calibration was determined spectrophotometrically at a wavelength of 240 nm with the molar extinction coefficient of 43,6 ($M^{-1} \times cm^{-1}$) [36]. Samples (3 ml) were put in polypropylene vials (Beckman, CIIIA) and added by 0,15 ml of "counting solution" containing PBS buffer1cM solution, pH 7.4, *p*-iodophenol, 50 μM, luminol, horse radish peroxidase, 10 nM when nanomolar concentrations of H_2O_2 were detected. "Counting solution" was prepared directly before the measurement. Due to the sensitivity of the method it is possible to determine H_2O_2 in a concentration of 0.1 nM [37].

Detection of OH-radical production was performed using coumarin-3-carboxylic acid (3-CCA). The product of 3-CCA hydroxylation, 7-hydroxycoumarin-3-carboxylic acid, is a suitable fluorescent probe for the detection of hydroxyl radicals [38]. A 0.5 мM solution of 3-CCA was prepared in water. Immediately before the measurement, a phosphate buffer (pH 7.4, 10 mM) is added to the excess solution to stabilize the pH. Fluorescence of 7-OH-CCA, formed as reaction of 3-CCA with hydroxyl radical, was measured using SRG laser spectrofluorometer where λ_{ex} = 405 nm, λ_{em} = 470 nm [39]. Due to the sensitivity of the method, it is possible to detect concentration of 7-OH-CCA of the order of 1 nM. Calibration was carried out both using commercial 7-OH-CCA (Sigma, United States) and after exposure to ionizing radiation at a dose of 0–100 Gy and then compared. Since the amount of hydroxyl radicals is estimated by a specific reaction with a dye, the concentration of hydroxyl radicals and their density in the volume can vary.

The content of nitrite and nitrate (NO_x) in samples was determined using the Griess reagent by the method described previously [40]. To determine the total concentrations of NO_x in specimens samples (100 μl) were introduced into the wells of a 96-well flat-bottom polystyrene plate, then a freshly prepared saturated solution (100 μl) of VCl_3 (8 g/L in 1 M HCl) was added and immediately after this 100 μl of the Griess reagent (1 M HCl containing 10 g/L of sulfanilamide and 1 g/L of N-1-naphthylethylenediamine hydrochloride) was introduced. The plate was kept at 37°C for 1 h and then the absorbance at 546 nm was measured with a plate reader Multiscan FC (TermoScintific, Finland). The content of nitrite was determined in a similar way but without the addition of VCl_3. For calibration, sodium nitrite and nitrate solutions of known concentration were used.

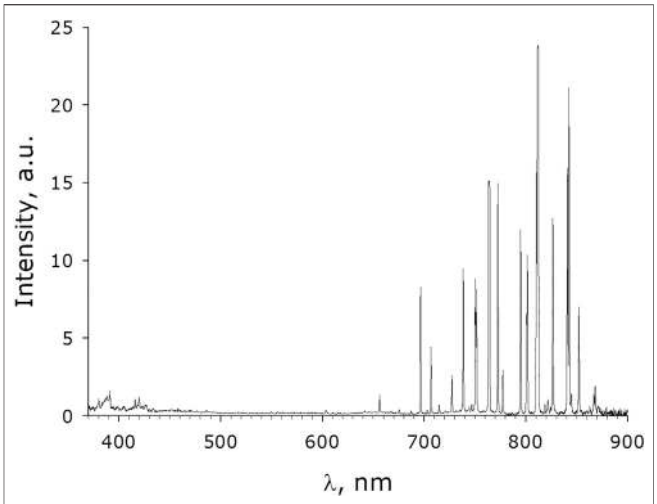

FIGURE 3 | Optical emission spectrum of the plasma jet, observed through the quartz wall of the experimental cell, measured when the plasma jet was immersed in water.

The concentration of molecular oxygen dissolved in water was measured using an AKPM-1-02 polarograph. The device has a sensitivity limit of 3 μM. The experimental measurement details were described previously [41]. The conductivity of the solutions was measured using a SanXin DDS-11C laboratory conductivity meter. The redox potential and pH were recorded using the EPV-1 sr and ESLK-13.7 electrodes connected to the Expert-001 measuring station. During the measurement, the water samples were mixed with a magnetic stirrer, its rotation speed 3 Hz [42].

Agrocultural Investigation

In the experiments, seeds of garden strawberry (Fragaria × ananassa) variety "Zenga Zengana" were used. One experiment used 100 seeds per group. Seed stratification took place at 3°C in relatively high humidity for 4°weeks. The seeds had a moisture content of about 7%, the average weight of one seed was about 300 μg. The seeds were germinated in Petri dishes with filter paper in the dark at a constant temperature of 20°C. PAW seed treatment was carried out at the beginning of seed germination. The plant length was measured on the 14th day of the experiments with an accuracy of 1 mm.

RESULTS

Emission spectrum of the plasma jet during the process of distilled water activation is shown in **Figure 3**. In the infrared region of spectrum (650–850 nm) there are a lot of bright lines of the excited argon (Ar I) and also the weak lines of ions Ar II (744, 750 nm) are present. In this part of the spectrum, except for argon lines, characteristic atomic lines of oxygen O (777нм) and hydrogen line H_α (656нм) are observed, but only at the presence of water and water vapors. In addition, weak lines of

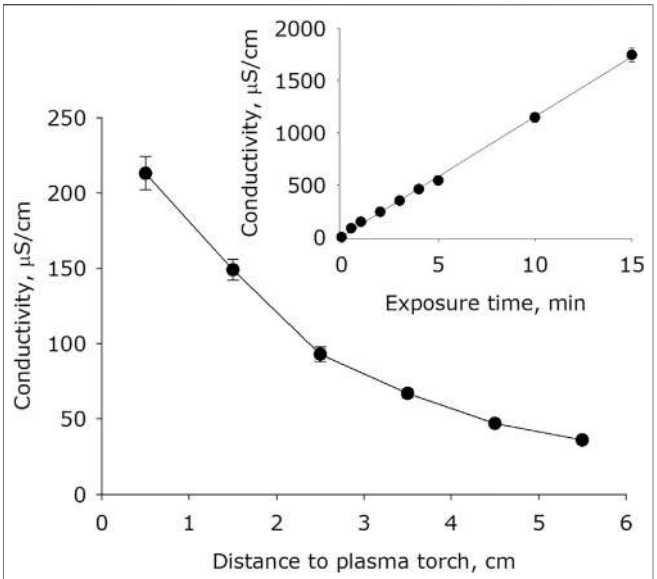

FIGURE 4 | The water electrical conductivity dependence on distance from water surface to the plasma jet nozzle at 1 min of plasma exposure. Data are presented as mean standard error for three independent experiments. Inset shows the water electrical conductivity depending on the time of plasma exposure at 1.5 cm distance from water surface to the plasma jet nozzle. The data are presented as average values with standard deviation of three experiment repetitions.

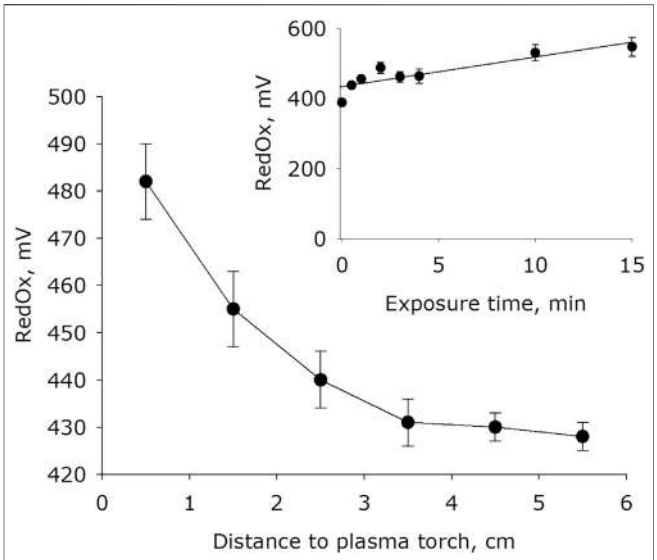

FIGURE 5 | The water redox potential dependence on distance from water surface to the plasma jet nozzle at 1 min of plasma exposure. Data are presented as mean standard error for three independent experiments. Inset shows the water redox potential depending on the time of plasma exposure at 1.5 cm distance from water surface to the plasma jet nozzle. The data are presented as average values with standard deviation of three experiment repetitions.

oxygen OI (715, 747, 795, 823, 844 nm) you can see there. In the blue part of the spectrum the following lines: argon ArI, ArII (near of 459 nm), nitrogen NI (746, 744, 762 nm), nitrogen ions NII (424, 460, 594 nm) and ionized oxygen OII (415, 459 nm) may be seen at high magnification. At much more magnification, it is possible also to see very weak the O_2^+ bands located along the entire length of the spectrum up to 790нм and bands of molecular oxygen O_2 before 437 nm. In the ultraviolet part of the spectrum, about 390°nm, overlapping weak bands of the O_2, O_2^+, NO, OH^+, and N_2 are observed. Similarly, in region 410 to 425 nm there is a superposition of the weak bands of the O_2; O_2^+, NO. Moderately intense emissions of the hydroxyl OH, and the argon ions Ar II could be observed in ultraviolet part of a spectrum at wavelengths less than 360 nm, which is placed outside of the spectrometer range. However, these spectra were shown in [43], where the conversion of water vapor in the DC-arc in argon-steam mixture was studied at atmospheric pressure.

It was shown that plasma exposure on water leads to a significant increase in its conductivity (**Figure 4**). The basic electrical conductivity of water after placing it in an experimental cell for 15 minutes is 0.9 μS × cm^{-1}. The dependence of the conductivity of water on the distance between the surface of the water and the plasma jet nozzle has a form close to a decaying exponential. For one minute of exposure, the water conductivity increases by 50–250 times depending on the distance. It was found that the water conductivity depends on the plasma exposure time linearly for at least 15 minutes. In this regard, the rate of increase in electrical conductivity at a distance between plasma and water of 0.5 cm is 220 μS × cm^{-1} × min-1, at a distance of 1.5 cm is 150 μS × cm^{-1} × min^{-1}, at 2.5 cm–90 μS × cm^{-1} × min^{-1}, at 3.5 cm–75 μS × cm^{-1} × min^{-1}, at 4.5 cm–50 μS × cm^{-1} × min^{-1}, at 5, 5 cm–40 μS × cm^{-1} × min^{-1}. The distance between plasma and water of 0.5 cm is minimal. In this case, the dynamic gas pressure of the plasma jet forms a pit in the water with a size of 1.5 cm in depth and a diameter of not more than 1.5 cm. With the distances shortening, the burning of the plasma jet becomes sharply turbulent with splashes of water from the pit and crackling noise. When the plasma torch is retired from the water to a distance of 1.5 cm, the burning of the jet becomes calm, the dynamic gas effect on water is minimal. This distance was chosen as the main one when measuring the characteristics of the plasma effect on water as a function of time.

It has been shown that plasma activation of water leads to an increase in the redox potential (**Figure 5**). The basic redox potential of water after placing it in an quartz cell for 15 minutes is 380 mV. The dependence of the value of the redox potential on the distance between the water surface and the plasma jet has the form close to a decaying exponential. In 1 minute of exposure, the redox potential of water increases by 15–25% depending on the jet distance. It was established that the redox potential of water changes with increasing plasma exposure time. The experimental results are approximated using a linear function (R^2 = 0.92).

It was shown that plasma exposure leads to a significant acidification of water, the value of the hydrogen index pH is decreased (**Figure 6**). The basic pH after placing water in an experimental cell for 15 minutes is 4.7. For 1 minute of exposure,

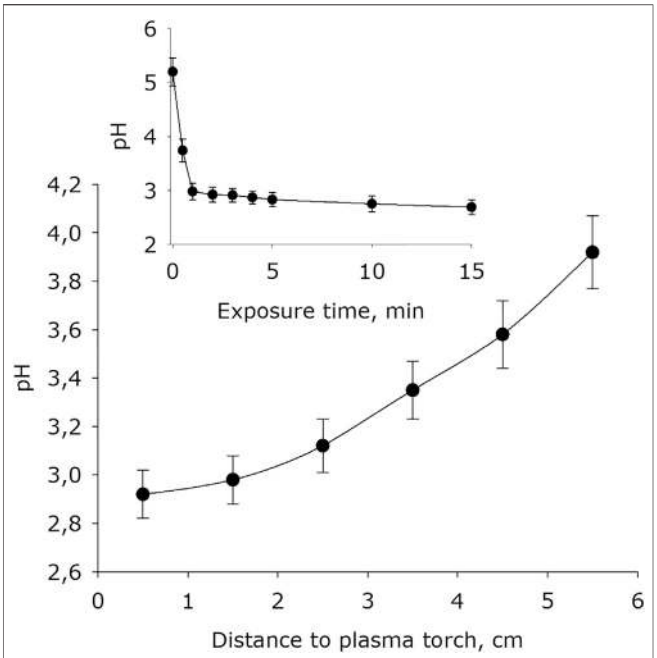

FIGURE 6 | The water pH-index dependence on distance from water surface to the plasma jet nozzle at 1 min of plasma exposure. Data are presented as mean standard error for three independent experiments. Inset shows the water pH-index depending on the time of plasma exposure at 1.5 cm distance from water surface to the plasma jet nozzle. The data are presented as average values with standard deviation of three experiment repetitions.

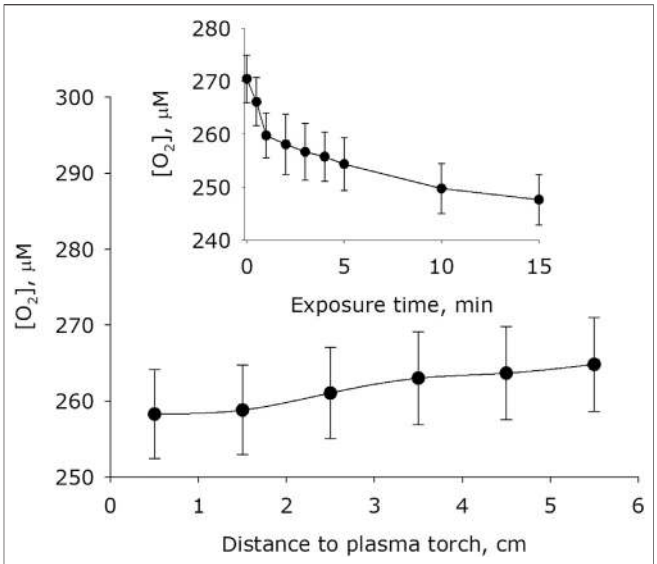

FIGURE 7 | Dependence of the concentration of oxygen dissolved in water on distance from water surface to the plasma jet nozzle at 1 min of plasma exposure. Data are presented as mean standard error for three independent experiments. Inset shows dependence of the concentration of oxygen dissolved in water on the time of plasma exposure at 1.5 cm distance from water surface to the plasma jet nozzle. The data are presented as average values with standard deviation of three experiment repetitions.

the water pH decreases by 0.7–1.7 units. With longer activation times, the pH index decreases at much lower rates. The dependence of the electrical conductivity of water on the distance between the water surface and the plasma jet nozzle has the form close to exponential decay. It was found that the water conductivity depending on plasma exposure time increases linearly.

It was shown that plasma activation of water leads to a change the molecular oxygen concentration dissolved in water (**Figure 7**). The basic concentration of molecular oxygen dissolved in water after placing water in an experimental cell for 15 minutes is 271 μM. Changes in the concentration of molecular oxygen dissolved in water weakly depends on the distance between the surface of the water and the plasma jet nozzle. Significant differences from the basic concentrations of molecular oxygen in water were obtained during plasma exposure for 1 minute on a distance 0.5 to 1.5 cm. It was found that the concentration of molecular oxygen dissolved in water decreases with the time of plasma exposure. In the first minute of treatment, it decreases by about 10 μM. When water is treated for 15 min from a distance of 1.5 cm, the concentration of molecular oxygen decreases by more than 20 μM.

It was shown that during plasma exposure to water intense formation of hydrogen peroxide occurs (**Figure 8**). The basic concentration of hydrogen peroxide in water 4 minutes after placing it in an experimental cell is 4 nM. The dependence of the rate of formation of hydrogen peroxide on the distance from

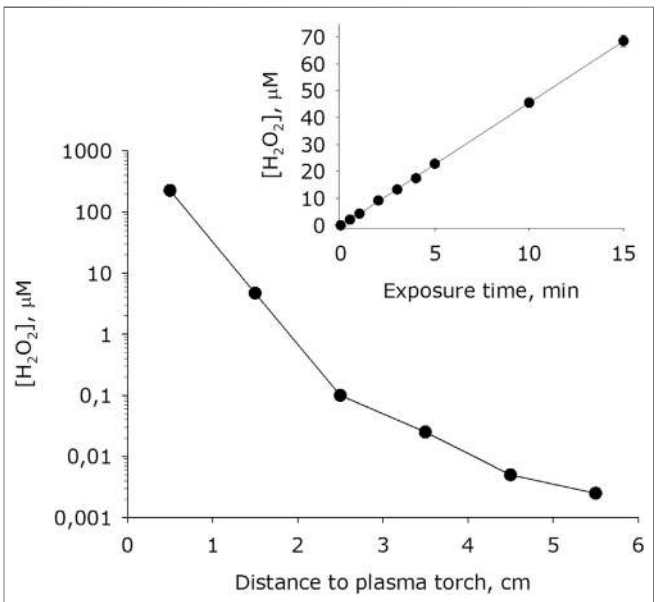

FIGURE 8 | Dependence of hydrogen peroxide concentration formed in water on distance from water surface to the plasma jet nozzle at 1 min of plasma exposure. Data are presented as mean standard error for three independent experiments. Inset shows dependence of hydrogen peroxide concentration formed in water on the time of plasma treatment at 1.5 cm distance from water surface to the plasma jet nozzle. The data are presented as average values with standard deviation of three experiment repetitions.

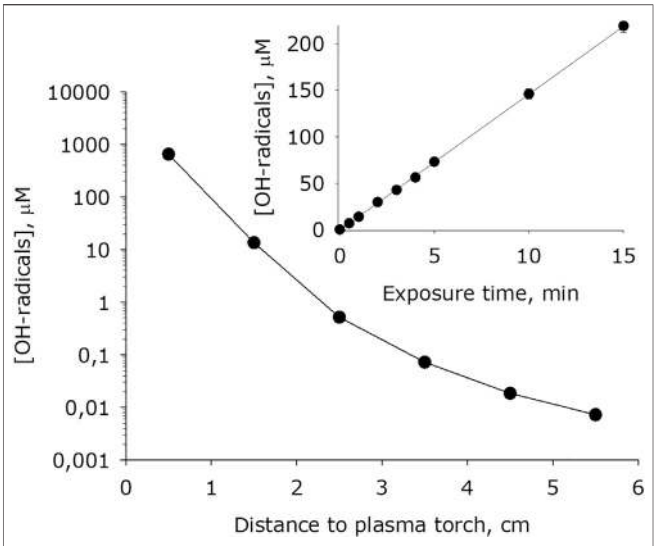

FIGURE 9 | Dependence of hydroxyl radicals concentration formed in water on distance from water surface to the plasma jet nozzle at 1 min of plasma exposure. Data are presented as mean standard error for three independent experiments. Inset shows dependence of hydroxyl radicals concentration formed in water on the time of plasma exposure at 1.5 cm distance from water surface to the plasma jet nozzle. The data are presented as average values with standard deviation of three experiment repetitions.

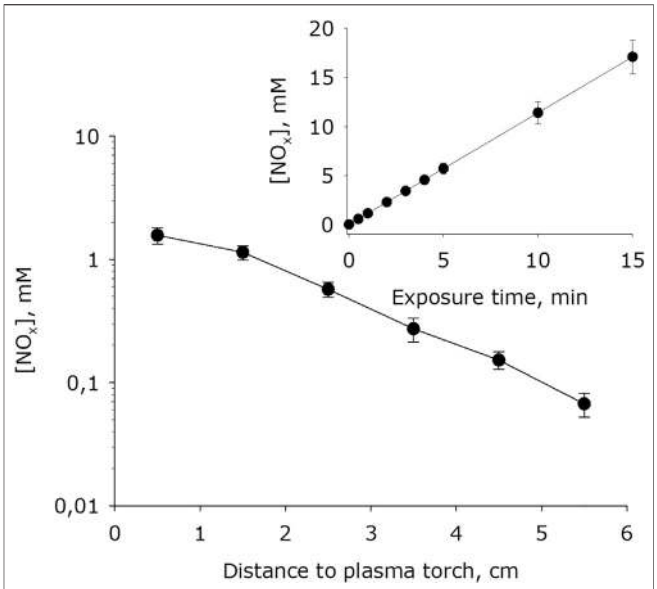

FIGURE 10 | Dependence of nitrite and nitrate anions concentration formed in water on distance from water surface to the plasma jet nozzle at 1 min of plasma exposure. Data are presented as mean standard error for three independent experiments. Inset shows dependence of nitrite and nitrate anions concentration formed in water on the time of plasma exposure at 1.5 cm distance from water surface to the plasma jet nozzle. The data are presented as average values with standard deviation of three experiment repetitions.

the water surface to the plasma jet nossle has the view like to an exponential decay. For one minute of plasma exposure the concentration of hydrogen peroxide in water increases by one to five orders of magnitude depending on the distance to the jet nozzle. It was found that the amount of hydrogen peroxide formed in water depends linearly on the time of plasma exposure for at least 15 minutes. Thereby, the rate of formation of hydrogen peroxide at a of 0.5 cm is 200 μM × min^{-1}, at a distance of 1.5 cm–50 μM × min^{-1}, at 2 5 cm–0. μM × min^{-1}, at 3.5 cm–50 nM× min^{-1}, at 4.5 cm–7 μM × min^{-1}, at 5.5 cm–4 μM × min^{-1}. In a series of experiments, quartz glass was placed between the plasma. Under the presented conditions, the rate of formation of hydrogen peroxide decreased by one and a half to two orders of magnitude.

It has been shown that at plasma exposure on water, an intensive formation of hydroxyl radicals occurs (**Figure 9**). The dependence of the of formation of hydroxyl radicals rate on the distance surface water to the plasma jet nozzle has the form close to an exponential decay. For 1 minute of treatment, the concentration of hydroxyl radicals in water increases by one to five orders of magnitude depending on the a distance of the water surface to the plasma jet nozzle. It was found that the amount of hydroxyl radicals formed in water depends linearly on the time of plasma exposure for at least 15 minutes.

It has been shown that, at plasma exposure on water, the intensive formation of nitrite and nitrate anions occurs (**Figure 10**). With increasing distance between the water surface and the plasma jet nozzle, the rate of formation of nitrite and nitrate anions decreases. It should be noted that the generation rate, depending on the distance changes in limits of one order of magnitude. It was also shown that the amount of nitrite and nitrate anions formed in water depends linearly on the time of plasma exposure for at least 15 minutes.

The effect of surfactants on the germination and development of strawberry seeds was studied. It was shown that strawberry seeds treated with PAW solution grow much faster than control seeds (**Figure 11**). The median size of control plants is in the order of 9 mm with a 95% confidence interval of 7.9 to 10.1 mm. The median size of PAW treated plants is in the order of 13 mm with a 95% confidence interval of 12.7 to 14.2 mm. Thus, PAW treated plants grow more than 40% faster than control plants.

DISCUSSION

It was found that the high-purity LT argon plasma, which has been got in an electrodeless microwave discharge at atmospheric pressure significantly changes the physicochemical properties of water (**Figures 4–10**). The overwhelming majority of installations receiving plasma using a magnetron cannot obtain high-purity plasma. In all the works known to us, the plasma is ignited either in a quartz tube [44, 45] or contacts the metal parts of the channel [46, 47]. The formation of such a chemically active molecule as hydrogen peroxide is observed. The nonequilibrium plasma of argon of the microwave jet in a medium of water vapor and

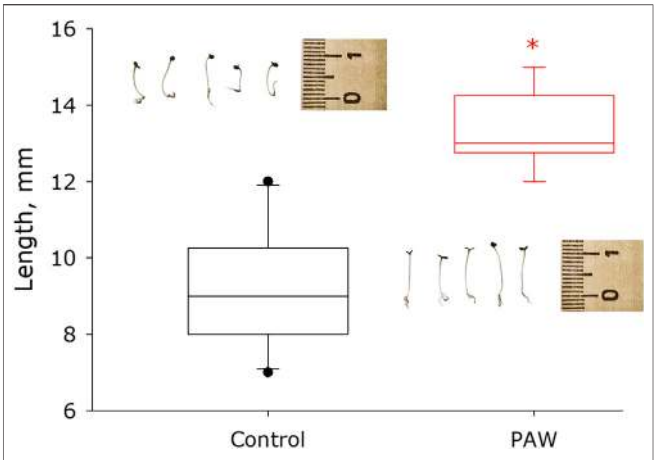

FIGURE 11 | Influence of plasma activated water solution on germination and development of seeds of garden strawberry. Data are presented as median with 95% confidence interval (box). The range is shown in the form of a whiskers. Statistically significant differences between control group and PAW groups (Mann-Whitney U test, $p < 0.05$) are marked by asterisks.

nitrogen (air) causes the decomposition of molecules into excited atoms and radicals [48]. Homolytic dissociation of water into a hydrogen atom and a hydroxyl radical is observed. The presence of excited hydrogen and oxygen atoms is demonstrated by the 656 nm line and the unresolved 777 nm line of the plasma emission spectrum (**Figure 3**). The formation of hydrogen peroxide under the action of plasma can obviously occur both in a vapor-air medium and in water. It was shown that when the plasma jet nozzle is displaced by 5 cm from the water surface, the yield of hydrogen peroxide decreases by five orders of magnitude (**Figure 8**). Obviously, for the intensive formation of hydrogen peroxide, the area and intensity of plasma exposure to water is critical. At the highest generation rate (at the distance 0.5 cm), approximately 99% of hydrogen peroxide is born in water, and the formation of hydrogen peroxide less than 1% takes place in the vapor-air medium. It is known that hydrogen peroxide can be formed in four ways (**Figure 12**):

(1) As a result of the recombination of hydroxyl radicals, which are formed during the homolytic dissociation of water [49]:$HO^{\bullet} + {}^{\bullet}OH \rightarrow H_2O_2$
Often the third body M participates in this reaction, since in its presence it is easier to explain the law of conservation of energy and momentum.

(2) When capturing hydrogen atoms by atmospheric oxygen molecules:
$H^{\bullet} + O_2 \rightarrow HO_2\bullet$
$HO_2^{\bullet} + HO_2^{\bullet} \rightarrow H_2O_2 + O_2$
In this case, hydroperoxide radicals are formed, the subsequent dismutation of which leads to the formation of hydrogen peroxide and molecular oxygen [50]. Sometimes molecular oxygen is formed in an excited state.

(3) Photolysis. High density plasma, such as the microwave Ar plasma, can produce a lot of UV radiation, which leads to the photolysis of water. The contribution of photolysis is difficult to separate from the direct exposure of plasma on water, seems, its effect on the surrounding gas-vapor medium

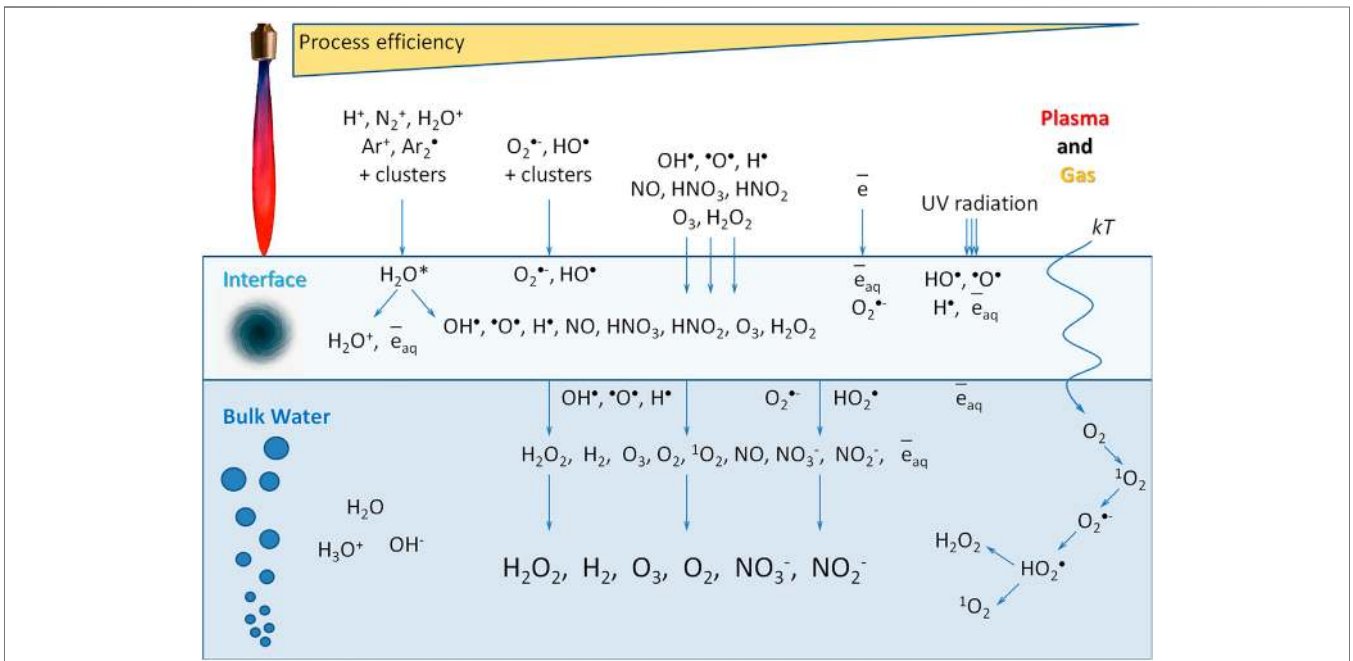

FIGURE 12 | Scheme of the main mechanisms of water activation under the action of plasma.

around a plasma jet to be essentially lower due to difference of vapor-water densities.

(4) The temperature mechanism of hydrogen peroxide generation [51, 52]:$O_2 + e + kT \rightarrow O_2^{\bullet -}$
$H^+ + O_2^{\bullet -} \rightarrow HO_2^{\bullet}$
$HO_2^{\bullet} + HO_2^{\bullet} \rightarrow H_2O_2 + O_2$ (at pH from 0.0 to 1.5, $k = 8.3 \times 10^5$).
$O_2^{\bullet -} + HO_2^{\bullet} + H^+ \rightarrow H_2O_2 + O_2$ (at pH = 4.8, $k = 9.7 \times 10^7$)

In this case, the transition of molecular oxygen from a triplet to a singlet state is observed, it reduces to a superoxide anion radical, which protonates in water with the formation of a hydroperoxide radical. Hydroperoxide radicals, in turn, also dismute with the formation of hydrogen peroxide. It was previously shown that under the action of heat, hydrogen peroxide is formed up to concentrations of several tens of nM [53]. This is a minor reaction that contributes at the level of tenths of a percent.

As our solutions were saturated with atmospheric gases, they contain carbon dioxide, which is partially converted to hydrogen carbonate anion in the solutions. Hydrogen carbonate anion is known to be a weak reducing agent and can have a significant effect on radical reactions. For example, it is widely known that hydrogen carbonate can affect the accumulation of hydrogen peroxide in water [54].

$HCO_3^- + OH^{\bullet} \rightarrow CO_3^{\bullet -} + H_2O$ ($k = 4 \times 10^7$)
$CO_3^{\bullet -} + OH^{\bullet} \rightarrow CO_2 + HO_2^-$ ($k = 3 \times 10^9$)
$CO_3^{\bullet -} + H_2O_2 \rightarrow HCO_3^- + HO_2^{\bullet}$ ($k = 8 \times 10^5$)

In addition, peroxynitrite, the formation of which is fundamentally possible under our conditions, will also react with hydrogen carbonate [55].

Obviously, such mechanism can significantly affect only when large distances between the plasma jet and the water surface is there. Two other mechanisms are fundamentally different each from other in the consumption of molecular oxygen. It was shown that the concentration of molecular oxygen in the system decreases (**Figure 7**). When the distance between the water surface and the plasma jet nozzle is 0.5 cm, approximately 200 μM hydrogen peroxide is formed per 1 minute and approximately 10 mM molecular oxygen is consumed. Taking into account the stoichiometry of chemical reactions, it can be argued that the first mechanism is responsible approximately for 95% of the total amount of hydrogen peroxide, and at the same time, when hydrogen atoms are captured by atmospheric oxygen molecules, no more than 5% of hydrogen peroxide molecules are formed. Thus, we can conclude that the generation of hydrogen peroxide occurs mainly in the aqueous phase due to the recombination of hydroxyl radicals. It should be noted that three molecules of hydroxyl radicals form one molecule of hydrogen peroxide. The same stoichiometry takes place when a water that does not contain impurities are exposed under radiation [51].

High-purity LT argon plasma of an electrodeless microwave discharge at atmospheric pressure creates nitrite and nitrate anions in water (**Figure 10**). The rate of generation of nitrite and nitrate anions, depending on the distance between the water surface and the plasma jet nozzle, changes by about one order of magnitude. The rate of generation of hydrogen peroxide and hydroxyl radical changes by about five orders of magnitude (**Figures 8**, **9**). That is, a change in the rate of generation of nitrite and nitrate anions against the background of the rates of H_2O_2 and OH-radicals practically does not noticible. This indirectly indicates that the generation of nitrite and nitrate anions occurs in a vapor-air medium. Nonequilibrium plasma causes the decomposition of not only water and oxygen molecules, but also nitrogen molecules. The resulting atoms interact, and in the course of annealing, nitrogen monoxide (NO) is formed in an ani-large yield. The presence of an unpaired electron in NO determines its tendency to manifest the properties of radicals, and therefore in radical reactions it is usually depicted as a radical ($NO^{\bullet}$). It is known that the formation of NO in air occurs at temperatures above 2100 K [56] and is associated with the absorption of a large amount of heat. With decreasing temperature, nitrogen monoxide in the reverse reaction decomposes into nitrogen and oxygen atoms. The half-life of NO in deionized water is inversely proportional to its concentration [57]. At concentrations in the range 0.05 to 1 μM, the half-life of NO can vary from 500 seconds to several hours [58]. It can be assumed that most of the formed NO manages to enter the reaction. It is believed that in the presence of molecular oxygen, nitrogen monoxide is oxidized to nitrogen dioxide (NO_2) by the reaction:

$2NO^{\bullet} + O \rightarrow 2NO_2^{\bullet}$

which, when dissolved in water, forms a mixture of nitrous and nitric acids:

$2NO_2^{\bullet} + H_2O \rightarrow HNO_2 + HNO_3$

Of course, there are alternative options for the oxidation of nitric oxide:

$NO^{\bullet} + HO_2^{\bullet} \rightarrow ONOOH$

For example, the reaction of NO with a hydroperoxide radical leads to the formation of peroxynitrite. Peroxynitrite at pH < pKa is often isomerized to nitrate form [59]. It is obvious that in water both nitric and nitrous acids dissociate into protons and nitrite or nitrate anions. The electrical conductivity of deionized water after placing it in an experimental cell for 15 min is 0.9 μS × cm^{-1}. The conductivity of hydrogen peroxide of 30% concentration is by several times greater only. The electrical conductivity of water for 15 minutes of plasma activation reaches 1700 μS × cm^{-1} (**Figure 4**). The specific conductivity of the nitric acid solution in the concentration range of 0.01–10 mM is approximately equal to 1 μS × cm^{-1}. Obviously, the conductivity is almost entirely due to the dissociation of molecules of nitric and nitrous acids. This is consistent with the fact that the pH of water with plasma treated for 15 min (**Figure 6**) also corresponds to these concentration of nitric and nitrous acids. Moreover, the obtained results also explain the change in the redox potential of the system (**Figure 5**).

Thus, the physicochemical properties of water activated by high-purity LT argon plasma of electrodeless microwave discharge at atmospheric pressure are established. At the maximum plasma–liquid contact area, it was shown that in the absence of impurities generation rate are 200 μM/min for

H_2O_2; 800 μM/min for $^{\bullet}OH$ and 2 mM/min for NO_x^-. Probably, this change in the chemical composition of the aqueous solution allows seeds to germinate faster and plants to develop more quickly (**Figure 11**).

CONCLUSION

The use of plasma-activated water (PAW) can be attributed to the number of global technological trends. Depending on the concentration of biologically active substances, PAWs may have both bactericidal properties and powerful stimulating properties. Contact methods for producing cold plasma and arc plasma are common today and introduce corrosion products of electrodes or dielectric surfaces into PAW. These products, on the one hand, can have a significant effect on both the biological properties of PAW and the conservation of biologically active substances in PAW. In this work, we presented a schematic diagram of a simple device for producing PAW without impurities. The device allows to change the properties of PAW in a wide range of properties and concentrations without losing cleanliness of PAW. Technologically, device requires a microwave generator (continuous, 0.9 kW) and sources of working gases at the inlet of the reactor (compressor (0.2 kW) or gas cylinder). The device is portable, easy to operate, accessible to any scientific laboratory or agricultural farm.

DATA AVAILABILITY STATEMENT

The original contributions presented in the study are included in the article/Supplementary Material, further inquiries can be directed to the corresponding author.

AUTHOR CONTRIBUTIONS

KS, AD, and SG were involved in conceptualization, investigation, writing—original draft, project management. NL, RS, AS, and IS. were involved in investigation.

FUNDING

This work was supported by a grant of the Ministry of Science and Higher Education of the Russian Federation for large scientific projects in priority areas of scientific and technological development (grant number 075-15-2020-774).

ACKNOWLEDGMENTS

The authors are grateful to the Center for Collective Use of the GPI RAS for the equipment provided.

REFERENCES

1. Weidinger A, Kozlov AV. Biological activities of reactive oxygen and nitrogen species: oxidative stress versus signal transduction. *Biomolecules* (2015) 5, 472–484. doi:10.3390/biom5020472
2. Hoeben WFLM, van Ooij PP, Lukes P, Leenders PHM, Huiskamp T, Pemen AJM. (2017) "Book of abstracts," in The 2017 IEEE pulsed power conference. Brighton, United Kingdom, June 18–June 22, 2017 [abstract] (2017).
3. Ganesh Subramanian PS, Jain A, Shivapuji AM, Sundaresan NR, Dasappa S, Rao L. Plasma-activated water from a dielectric barrier discharge plasma source for the selective treatment of cancer cells. *Plasma Process Polym.* (2020) 17, 1900260. doi:10.1002/ppap.201900260
4. Kurake N, Tanaka H, Ishikawa K, Takeda K, Hashizume H, Nakamura K, et al. Effects of ·OH and ·NO radicals in the aqueous phase on H_2O_2 and NO_2– generated in plasma-activated medium. *J. Phys. D. Appl. Phys.* (2017) 50, 155202. doi:10.1088/1361-6463/aa5f1d
5. Thirumdas R, Kothakota A, Annapure U, Siliveru K, Blundell R, Gatt R., et al. Plasma activated water (PAW): chemistry, physico-chemical properties, applications in food and agriculture. *Trends Food Sci. Technol.* (2018) 77, 21–31. doi:10.1016/j.tifs.2018.05.007
6. Davidson PM, Sofos JN, Branen, AL. *Antimicrobials in food*. 3rd Edn. Boca Raton, FL: CRC Press (2005).
7. Sharma S, Yadav S, Sibi G. Accrediting gene therapies with non-viral lipid nanoparticles delivery system and its related pertinence. *J Crit. Rev.* (2020) 7, 11–15. doi:10.22159/jcr.07.01.02
8. Andreev SN, Apasheva LM, Ashurov MX, Lukina NA, Sapaev B., Sapaev IB, et al. Production of pure hydrogen peroxide solutions in water activated by plasma of an electrodeless microwave discharge and their application for controlling plant growth. *Dokl Phys.* (2019) 64, 222–224. doi:10.1134/S1028335819050094
9. Lamichhane JR, Dürr C, Schwanck AA, Robin MH, Sarthou JP, Cellier V, et al. Integrated management of damping-off diseases. a review. *Agron Sustain Dev* (2017) 37:10. doi:10.1007/s13593-017-0417-y
10. Winter J, Brandenburg R, Weltmann K-D. Atmospheric pressure plasma jets: an overview of devices and new directions. *Plasma Sources Sci Technol* (2015) 24, 064001. doi:10.1088/0963-0252/24/6/064001
11. Laroussi M, Lu X, Keidar M. Perspective: the physics, diagnostics, and applications of atmospheric pressure low temperature plasma sources used in plasma medicine. *J Appl Phys* (2017) 122, 020901. doi:10.1063/1.4993710
12. Lu XP, Reuter, S, Laroussi, M, Liu, DW. *Nonequilibrium atmospheric pressure plasma jets: fundamentals, diagnostics, and medical applications*. Boca Raton, FL: CRC Press (2019).
13. Piskarev IM, Ivanova IP, Trofimova, SV. Chemical effects of self-sustained spark discharge: simulation of processes in a liquid. *High Energy Chem.* (2013) 47, 62–66. doi:10.1134/S0018143913020082
14. Tian Y, Ma R, Zhang Q, Feng H, Liang Y, Zhang J, et al. Assessment of the physicochemical properties and biological effects of water activated by non-thermal plasma above and beneath the water surface. *Plasma Process Polym* (2015) 12, 439–449. doi:10.1002/ppap.201400082
15. Piskarev IM, Ivanova IP, Trofimova SV, Ichetkina AA, Burkhina OE. Formation of peroxynitrite induced by spark plasma radiation. *High Energy Chem.* (2014) 48, 213–216. doi:10.1134/S0018143914030138
16. Ahmed MW, Choi S, Lyakhov K, Shaislamov U, Mongre RK, Jeong DK, et al. High-frequency underwater plasma discharge application in antibacterial activity. *Plasma Phys Rep* (2017) 43, 381–392. doi:10.1134/S1063780X17030011
17. Lu P, Boehm D, Bourke P, Cullen PJ. Achieving reactive species specificity within plasma activated water through selective generation using air spark and glow discharges. *Plasma Process Polym.* (2017) 14, 1600207. doi:10.1002/ppap.201600207
18. Raizer YP. *Gas discharge physics*. Editor Allen JE (Heidelberg: Springer-Verlag Berlin Heidelberg) (2012).
19. Lieberman MA, Lichtenberg AJ. *Principles of plasma discharges and materials processing*. 2nd Edn. Hoboken, NJ, United States: Wiley-Interscience (2005)
20. Chu PK, Lu XP. *Low temperature plasma technology: methods and applications*. Boca Raton, FL, United States: CRC Press, 493 (2013).

21. Ohta T. "8 plasma in agriculture," in *Cold plasma in food and agriculture: fundamentals and applications*. editors Misra NN, Schluter O, Cullen PJ (Cambridge, United Kingdom: Academic Press), (2016). 205–221.
22. Thirumdas R, Kothakota A, Annapure U, Siliveru K, Blundell R, Gatt R, et al. Plasma activated water (PAW): chemistry, physico-chemical properties, applications in food and agriculture. *Trends Food Sci. Technol.* (2018) 77, 21–31. doi:10.1016/j.tifs.2018.05.007
23. Ito M, Oh JS, Ohta T, Shiratani M, Hori M. Current status and future prospects of agricultural applications using atmospheric-pressure plasma technologies. *Plasma Process Polym* (2018) 15, 1700073. doi:10.1002/ppap.201700073
24. Laroussi M, Kong MG, Morfill G. *Plasma medicine*. Cambridge, United Kingdom: Cambridge University Press, (2012). 346
25. Fridman A, Friedman G. *Plasma medicine*. Chichester, United Kingdom: John Wiley & Sons, (2012). 592.
26. Toyokuni S, Ikehara Y, Kikkawa F, Hori M. *Plasma medical science*. Cambridge, United Kingdom: Academic Press, (2018) 458.
27. Kolb JF, Mohamed A-AH, Price RO, Swanson RJ, Bowman A, Chiavarini RL, et al. Cold atmospheric pressure air plasma jet for medical applications. *Appl Phys. Lett.* (2008) 92, 241501. doi:10.1063/1.2940325
28. Liu J, He B, Chen Q, Li J, Xiong Q, Yue G, et al. Direct synthesis of hydrogen peroxide from plasma-water interactions. *Sci Rep* (2016) 6, 38454. doi:10.1038/srep38454
29. Xu H, Liu D, Wang W, Liu Z, Guo L, Rong M, et al. Investigation on the RONS and bactericidal effects induced by He + O_2 cold plasma jets: in open air and in an airtight chamber. *Phys Plasmas* (2018) 25, 113506. doi:10.1063/1.5055802
30. Koppenol WH. The centennial of the Fenton reaction. *Free Radic Biol Med* (1993) 15, 645–651. doi:10.1016/0891-5849(93)90168-t
31. Brandenburg R. Corrigendum: dielectric barrier discharges: progress on plasma sources and on the understanding of regimes and single filaments Plasma Sources. *Sci Tech* (2017) 26, 053001. doi:10.1088/1361-6595/aaced9
32. Dobrynin D, Friedman G, Fridman A, Starikovskiy A. Inactivation of bacteria using dc corona discharge: role of ions and humidity. *New J Phys* (2011) 13, 103033. doi:10.1088/1367-2630/13/10/103033
33. Jones BT, Hou X. "Inductively coupled plasma/optical emission spectrometry," in *Encyclopedia of analytical chemistry*. editor Meyers R. A., (Chichester, UK: John Wiley & Sons), (2000) 9468–9485.
34. Sergeichev KF, Lukina NA, Arutyunyan NR. Atmospheric-pressure microwave plasma torch for CVD technology of diamond synthesis. *Plasma Phys. Rep.* (2019) 45, 551–560. doi:10.1134/S1063780X19060096
35. Gudkov SV, Penkov NV, Baimler IV, Lyakhov GA, Pustovoy VI, Simakin AV, et al. Effect of mechanical shaking on the physicochemical properties of aqueous solutions. *Int J Mol Sci* (2020) 21, 8033. doi:10.3390/ijms21218033
36. Ermakov A, Ermakova O, Skavulyak A, Kreshchenko N, Gudkov S, Maevsky E. The effects of the low temperature argon plasma on stem cells proliferation and regeneration in planarians. *Plasma Process Polym* (2016) 13, 788–801. doi:10.1002/ppap.201500203
37. Shtarkman IN, Gudkov SV, Chernikov AV, Bruskov VI. Effect of amino acids on X-ray-induced hydrogen peroxide and hydroxyl radical formation in water and 8-oxoguanine in DNA. *Biochemistry Mosc* (2008) 73, 470–478. doi:10.1134/S0006297908040135
38. Manevich Y, Held KD, Biaglow JE. Coumarin-3-carboxylic acid as a detector for hydroxyl radicals generated chemically and by gamma radiation. *Radiat Res* (1997) 148, 580–591.
39. Gudkov SV, Guryev EL, Gapeyev AB, Sharapov MG, Bunkin NF, Shkirin AV, et al. Unmodified hydrated C. *Nanomedicine* (2019) 15, 37–46. doi:10.1016/j.nano.2018.09.001
40. Miranda KM, Espey, MG, Wink, DA. A rapid, simple spectrophotometric method for simultaneous detection of nitrate and nitrite. *Nitric Oxide Biol Chem* (2001) 5, 62–71. doi:10.1006/niox.2000.0319
41. Simakin AV, Astashev ME, Baimler V, Uvarov OV, Voronov VV, Vedunova MV, et al. The effect of gold nanoparticle concentration and laser fluence on the laser-induced water decomposition. *J. Phys. Chem. B* (2019) 123, 1869–1880. doi:10.1021/acs.jpcb.8b11087
42. Chernikov AV, Gudkov SV, Shtarkman IN, Bruskov VI. Oxygen effect in heat-mediated damage to DNA. *Biofizika* (2007) 52, 244–51. doi:10.1134/S0006350907020078
43. Park C. Hydrogen line ratios as electron temperature indicators in nonequilibrium plasmas. *J Quant. Spectrosc. Radiat. Transfer* (1971) 12, 323–370. doi:10.1016/0022-4073(72)90050-7
44. Miotk R, Hrycak B, Jasiński M, Mizeraczyk J. Characterization of an atmospheric-pressure argon plasma generated by 915 MHz microwaves using optical emission spectroscopy. *J Spectroscopy* (2017) 2017, 6359107. doi:10.1155/2017/6359107
45. Isoldi M, Ozono EM, Mansano RD. Excitation temperature measurements on a new atmospheric microwave plasma torch. *J Nanosci Nanoeng Appl* (2018) 2, 105.
46. Choi J., Eom IS, Kim V, Kwon YW, Joh HM, Jeong BS, et al. Characterization of a microwave-excited atmospheric-pressure argon plasma jet using two-parallel-wires transmission line resonator. *Phys Plasmas* (2017) 24, 093516. doi:10.1063/1.4989728
47. Jasinski M, Mizeraczyk J. Plasma sheet generated by microwave discharge at atmospheric pressure. *IEEE Trans Plasma Sci* (2011) 39, 2136–2137. doi:10.1109/TPS.2011.216200
48. Weltmann K-D, Kolb JF, Holub M, Uhrlandt D, Šimek M, Ostrikov K, et al. The future for plasma science and technology. *Plasma Process Poly* (2019) 16, 1800118. doi:10.1002/ppap.201800118
49. Qi Z, Zhang Q, Zhu D, Ding Z, Niu J, Liu D, et al. The reaction pathways of H_2O_2(aq) in the He plasma jet with a liquid system. *Plasma Chem Plasma Process* (2020) 40, 100–1018. doi:10.1007/s11090-020-10065-3
50. Ivanov VE, Usacheva AM, Chernikov AV, Bruskov VI, Gudkov SV. Formation of long-lived reactive species of blood serum proteins induced by low-intensity irradiation of helium-neon laser and their involvement in the generation of reactive oxygen species. *J Photochem Photobiol B* (2017) 176, 36–43. doi:10.1016/j.jphotobiol.2017.09.012
51. Ward JF. DNA damage produced by ionizing radiation in mammalian cells: identities, mechanisms of formation, and reparability. *Prog Nucleic Acid Res Mol Biol* (1988) 35, 95–125. doi:10.1016/s0079-6603(08)60611-x
52. Sheng Y, Abreu IA, Cabelli DE, Maroney MJ, Miller AF, Teixeira M, et al. Superoxide dismutases and superoxide reductases. *Chem Rev* (2014) 114, 3854–3918. doi:10.1021/cr4005296
53. Bruskov VI, Malakhova LV, Masalimov ZK, Chernikov AV. Heat-induced formation of reactive oxygen species and 8-oxoguanine, a biomarker of damage to DNA. *Nucleic Acids Res* (2002) 30, 1354–1363. doi:10.1093/nar/30.6.1354
54. Belovolova LV. Reactive oxygen species in aqueous media (A review). *Optic Spectrosc* (2020) 128, 932–951. doi:10.1134/S0030400X20070036
55. Bruskov VI, Chernikov AV, Ivanov VE, Karmanova EE, Gudkov SV. Formation of the reactive species of oxygen, nitrogen, and carbon. *Phys Wave Phenom* (2020) 28, 103–106. doi:10.3103/S1541308X2002003X
56. Zeldovich YB. The oxidation of nitrogen combustion and explosions. *Acta Physicochim.* (1946) 21, 577–628.
57. Wink DA, Darbyshire JF, Nims RW, Saavedra JE, Ford PC. Reactions of the bioregulatory agent nitric oxide in oxygenated aqueous media: determination of the kinetics for oxidation and nitrosation by intermediates generated in the NO/O2 reaction. *Chem Res Toxicol* (1993) 6, 23–7. doi:10.1021/tx00031a003
58. Ignarro LJ, Fukuto JM, Griscavage JM, Rogers NE, Byrns RE. Oxidation of nitric oxide in aqueous solution to nitrite but not nitrate: comparison with enzymatically formed nitric oxide from L-arginine. *Proc Natl Acad Sci U. S. A.* (1993) 90, 8103–8107. doi:10.1073/pnas.90.17.8103
59. Kissner R, Koppenol WH. Product distribution of peroxynitrite decay as a function of pH, temperature, and concentration. *J Am Chem Soc* (2002) 124, 234–9. doi:10.1021/ja010497s

Conflict of Interest: The authors declare that the research was conducted in the absence of any commercial or financial relationships that could be construed as a potential conflict of interest.